Ancient TL

www.ancienttl.org · ISSN: 2693-0935

Bossin, L. and King, G., 2021. *Constraining heterogeneity in the absorbed dose of 50 keV X-ray irradiated samples for EPR dating: simulation and experimental approaches.* Ancient TL 39(2): 1-11. https://doi.org/10.26034/la.atl.2021.551

This article is published under a *Creative Commons Attribution 4.0 International* (CC BY): https://creativecommons.org/licenses/by/4.0

© The Author(s), 2021

licensed under CC BY 4.0

Ancient TL

Constraining heterogeneity in the absorbed dose of 50 keV X-ray irradiated samples for EPR dating: simulation and experimental approaches

Lily Bossin[1,2*] and Georgina King[1]

[1] Institute of Earth Surface Dynamics, University of Lausanne, Switzerland
[2] Current address: Department of Radiation Safety and Security, Paul Scherrer Institute, Villigen, Switzerland

*Corresponding Author: lily.bossin@psi.ch

Received: December 18, 2020; in final form: November 19, 2021

Abstract

X-band Electron Paramagnetic Resonance (EPR) of quartz requires the irradiation of samples with volumes of ca 3 mm^3, which can be conveniently achieved using commercially available instruments such as the 50 keV X-ray Dose manufactured by Freiberg Instruments. However, X-rays at such low energies can result in highly heterogeneous absorbed doses. In this contribution we use Monte-Carlo particle transport simulations (MCNP6) to characterise the heterogeneity of the radiation field in a 3 mm inner-diameter EPR sample tube irradiated using a 50 kV X-ray generator. From these simulations, we demonstrate that the use of an aluminium filter (200 µm) is redundant when irradiating samples in glass tubes (500 µm wall thickness). Simulations of grain-by-grain absorbed doses across the tubes indicate a maximum of 20 % axial heterogeneity for grains at the tube centre, even when the sample is rotated throughout irradiation. Single-grain luminescence dosimetry measurements were used to experimentally validate the heterogeneity predicted, confirming the modelling results. EPR dosimetry calibration of the X-ray source yielded a dose rate of 0.206 ± 0.005 Gy·s^{-1}.

Keywords: EPR, X-ray source, Calibration, Monte-Carlo simulations

1. Introduction

Continuous-Wave Electron Paramagnetic Resonance (CW-EPR) X-band measurements of granular quartz require the irradiation of significant masses of material (ca 60 mg). X-ray sources can be used for this purpose. X-ray sources are relatively inexpensive and raise fewer safety concerns compared with radionuclide sources. It is thus practical to have them within an individual EPR laboratory. In contrast, gamma sources are generally restricted to specialised institutions requiring samples to be transported for irradiation and precluding single-aliquot investigations (e.g. Tsukamoto et al. 2015). X-ray sources have already been used to reconstruct the geological dose of natural minerals using luminescence techniques (Andersen et al. 2003; Thomsen et al. 2006; Kook et al. 2011; Richter et al. 2016) and more recently have been proposed for the irradiation of samples for EPR dating of natural quartz (Oppermann & Tsukamoto, 2015). Studies have also highlighted the advantages of using X-ray sources for luminescence dating; earlier work from Andersen et al. (2003) has shown that the Varian VF-50J X-ray tube (V_{max} = 50 keV) could be used for luminescence dating of quartz with satisfactory linearity between dose rate and current, meaning that dose rate adjustment could easily be achieved by varying the current. The authors also found that the X-ray tube exhibited good stability over time, yielding little variation in dose-rate throughout irradiation or with usage time, and yielded good dose recovery results. This was later confirmed by Thomsen et al. (2006) and Richter et al. (2016).

However, two major challenges affect the routine use of low energy (< 100 keV) X-ray sources for trapped-charge dosimetry: 1) variability in absorbed dose between minerals of the same type, but with different origins for identical irradiation time, operating voltage and current (Thomsen et al., 2006), 2) dependency of the absorbed dose-rate on the sam-

ple's thickness, due to strong absorption and 3) heterogeneity in absorbed dose for bulky samples such as those used in EPR dating. The first challenge was identified for natural quartz and was attributed to micro-dosimetric effects. Although quartz is one of the purest minerals on earth, a number of defects and impurities occur in natural quartz minerals (Götze & Lewis, 1994). The concentration and nature of these defects is highly variable between different quartz samples, which is reflected in the variability of their respective EPR and luminescence responses (Beerten & Stesmans 2007; Duller et al. 2000). Thomsen et al. (2006) showed that X-ray dose-rate heterogeneity for grains of quartz deposited on stainless steel discs could be reduced by using a 200 µm aluminium filter to harden the X-ray spectrum (shifting the mean emission from ~ 10 keV to ~ 15 keV; Richter et al. 2016). Richter et al. (2016) showed that hardening the beam led to an increase in the penetration depth, thus ensuring a homogeneous irradiation of the grains, although consequently the total dose-rate was reduced.

This study addresses the second challenge, that the dose to bulky samples can be highly heterogeneous. Previous work has shown that irradiation using a 50 keV Varian VF-50J X-ray tube can be used to irradiate samples within their measurement tube, thus paving the way towards single-aliquot regenerative dose protocols for EPR dating (Tsukamoto et al., 2015). Oppermann & Tsukamoto (2015) measured a radial heterogeneity of 3.1 % for samples 1.5 cm high using GaF chromic films. By comparing the dose assessed using GaF chromic films with and without a sample tube, they also predicted an axial reduction in dose to quartz of 35 % at the centre of 3 mm diameter tubes. Oppermann & Tsukamoto (2015) finally reported a reproducibility within 20 % for their setup, using X-ray irradiated alanine dosimeters.

To complement these studies and to calibrate the X-ray source recently installed at the University of Lausanne we employed radiation-transport simulations (MCNP6) to calculate the absorbed dose to grains of quartz irradiated in EPR sample tubes using a Varian VF-50J X-ray source (Tungsten target, operated at 50 keV). Radiation-transport codes such as MCNP or GEANT have already been used to characterise the artificial-laboratory-induced dose delivered to samples in instruments designed for trapped charge dating. This is because a simulation approach allows dose deposition to be investigated at a scale not achievable by experimental means. This includes, for example, the dose-depth profiles in sliced samples (Bailiff, 2018) or the evaluation of the backscatter component of samples of various shapes irradiated in a luminescence reader (Autzen et al. 2017).

In the first part of this paper, a simulation-based approach is used to determine the deposition energy spectrum for different filtering conditions to evaluate whether the spectrum needs to be filtered with, for example, an aluminium filter. Dose attenuation through the tube is then simulated at a single-grain level, a level of precision not achievable using experimental procedures. These simulations serve as the basis for the X-ray generator calibration, allowing more accurate error estimation and a better understanding of how dose is distributed within a sample tube. In the second part of this paper, optically stimulated luminescence (OSL) single-grain measurements of quartz grains irradiated with the X-ray source are used to experimentally assess absorbed dose heterogeneity and to either falsify or verify the MCNP results. Finally, EPR dosimetry of granular quartz is used to calibrate the source for quartz grains in the grain size fraction 180 – 212 µm.

2. Materials and Methods

2.1. Description of the X-ray source and irradiation geometry

The X-ray apparatus "X-ray dose" manufactured by Freiberg Instruments (Figure 1) comprises a Varian VF-50J X-ray source (tungsten target, Beryllium window 76 µm) coupled to a Spellman power supply operating at a maximum voltage V_{max} = 50 keV, and maximum current I_{max} = 1 mA. A rotating sample tube holder is incorporated to provide better homogeneity during sample irradiation. The sample tube is placed 40 mm from the end of the X-ray tube during irradiation and the beam is collimated to provide a restricted irradiation window. A 9 mm thick brass shutter (maximum shutter time 300 ms) controls the beginning and end of the irradiation and allows irradiation to start only when the tube has warmed up and reached the desired voltage and current. Documentation on the instrumentation is available from the manufacturer ("X-ray dose manual", available on demand from Freiberg Instruments). The samples are irradiated in glass sample tubes (Wilmad Suprasil) of 3 mm external diameter and 2 mm internal diameter (glass thickness: 500 µm).

2.2. Radiation-transport simulations

A simplified model of the irradiation geometry was built in MCNP6.2 (Goorley et al., 2012), comprising a plan parallel source with an emission energy spectrum taken from Richter et al. (2016). This spectrum mimics the emission spectrum for the unfiltered X-ray source operating at a voltage of 50 keV. The beam was not collimated in these simulations, as the exact geometry of the collimator was not known.

The grains of quartz were modelled as 200 µm diameter SiO_2 spheres of density g = 2.63 g·cm^{-3}. The glass tube (SiO_2, density g = 2.2 g·cm^{-3}) was filled with these grains using an MCNP repeated structure following a cubic lattice and placed 40 mm from the plan parallel source (Figure 2). The geometry was simulated in air.

The Monte Carlo N-Particle Transport version 6 (MCNP6, Goorley et al. 2012; Pelowitz 2013) code developed by Los Alamos National Laboratory was used to simulate the transport and interactions of particles using repeated random processes. The behaviour of each particle is simulated and recorded in specific volumes (cells). Results are reported using "tallies" that count the number of specified events (e.g., track length, collision, surface crossing) in a given cell. MCNP can calculate the absorbed dose in a cell using the energy deposition tally (F6 tally) or the pulse height

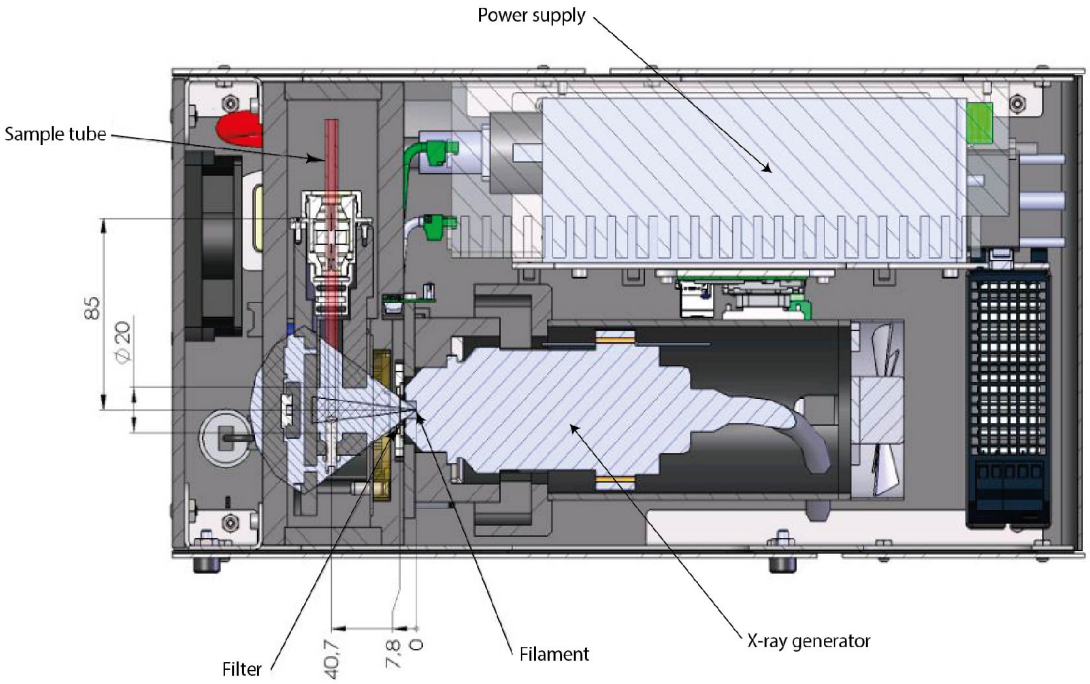

a)

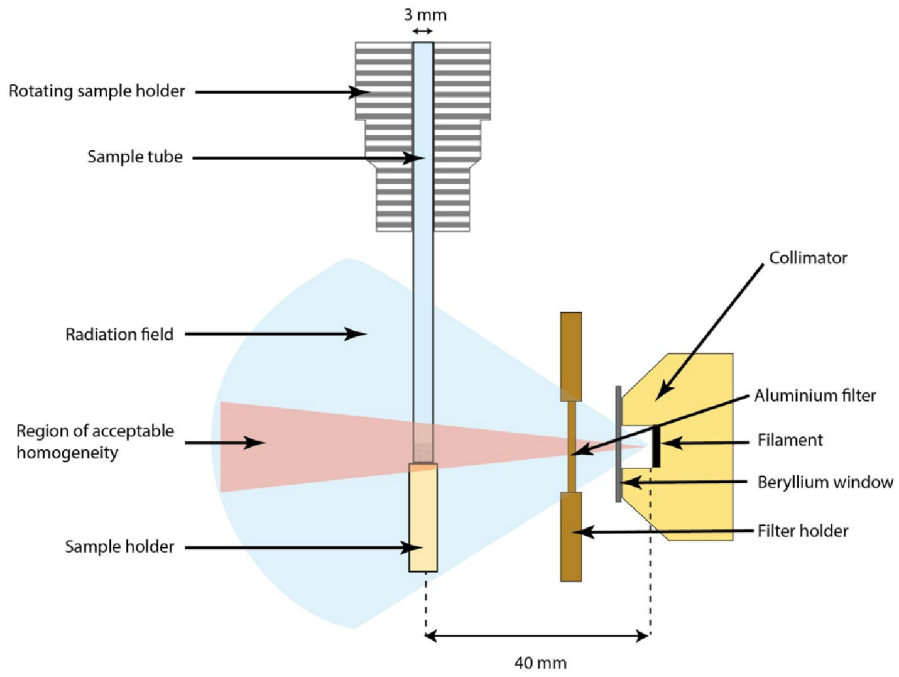

b)

Figure 1. Schematic representation of the "X-ray dose"; a) figure taken from the Freiberg Instrument manual representing the entire apparatus and b) figure of the sample tube positioning during irradiation. Redrawn from the Freiberg Instrument manual (figure not to scale). The region of acceptable homogeneity is arbitrarily defined as the region within which the radial variation in absorbed dose is less than 5 %.

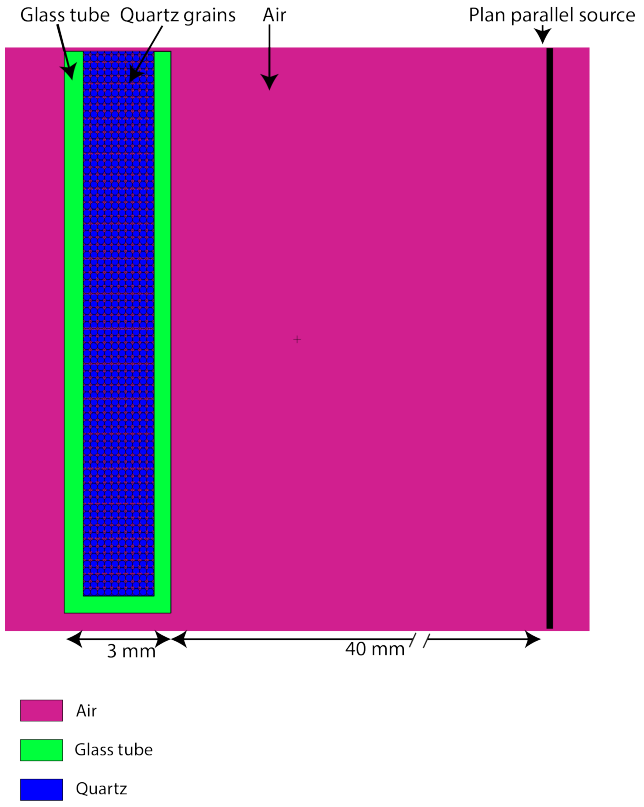

Figure 2. Geometry employed to model the irradiation of samples of granular quartz inside a glass sample tube with the Freiberg Instruments X-ray generator "X-ray dose". The geometry was plotted using the MCNP plotter and later modified.

in a cell times the energy deposited (*F8 tally). The code was run until all 10 MCNP statistical checks converged - evaluating the mean error, the variance, the variation of the figure of merit and the slope of the probability density function. The errors indicated are MCNP statistical errors only and thus do not include the systematic errors inherent to the simulation of an experimental setup. Where necessary, the errors were propagated using a Monte-Carlo procedure implemented in the software Matlab.

Sample name	**Origin**
KRG113	Granitic bedrock, Japanese Alps
NUS18	Sandy limestone, Al Wafa site (28°00′58.4″N, 10°47′52.3″E), Lybia
RisøCalQz0Gy	Quartz sand, Rømø, Denmark (Hansen et al., 2015)

Table 1. List of samples selected to calibrate the X-ray source with their origin

2.3. Luminescence dosimetry

Three quartz samples of different origins (listed in Table 1) were selected to experimentally quantify the absorbed dose heterogeneity of an individual EPR aliquot irradiated with the X-ray source. The samples were prepared using standard methods to extract the granular quartz fraction in the range 180 – 212 µm. The samples were subjected to a thermal treatment (400 °C, 4 min) to zero the signal and then irradiated for 100 s in EPR glass samples tubes (3 mm outside diameter, 2 mm inside diameter) using the X-ray source operating at a voltage of 50 keV and a current of 1 mA. No filters were used when irradiating the samples, as Section 3 will show that the use of filters was not necessary in our setup.

The resulting absorbed dose in the grains of quartz was measured using optically simulated luminescence (OSL) methods. The measurements were performed using a Risø model 20 reader (DTU Nutech, Denmark) that incorporated a ^{90}Sr/^{90}Y β radiation source. The luminescence emission was detected through a UV pass colour glass filter (U-340) using an Electron Tube 9235Q PMT (160 – 630 nm). The β source of the luminescence reader was calibrated using quartz irradiated with a ^{137}Cs γ source at DTU Nutech, whose dose-rate to grains of quartz is calibrated and characterised (Hansen et al., 2015) and was evaluated to deliver 0.091 ± 0.007 Gy·s^{-1} to grains mounted on single-grain aluminium discs, at the date of measurement. The β dose-rate was corrected for the heterogeneity of the source across the single-grain measurement discs. The absorbed dose to grains of quartz was determined by applying a single aliquot regenerative dose procedure (SAR; Murray & Wintle 2000) using a 10 s Nd:YVO_4 solid-state diode-pumped laser light stimulation (532 nm; with a power at the sample position of 10 mW·cm^{-2} as stated by the manufacturer at the time of purchase; Bøtter-Jensen et al. 2000), a 260 °C preheat (10 s hold time) and holding the samples at 125 °C during the OSL measurement. Unless otherwise specified, the rejection criteria applied included a maximum X-ray dose and test dose (18 Gy) error of 10 % and a recycling ratio < 0.1. β dose-recovery tests carried out on 12 further aliquots of the same samples, following thermal annealing and administration of a β dose of 11.8 ± 0.9 Gy, indicated that this protocol was suitable to recover doses within 3%. These experiments also served to constrain the sample-specific intrinsic OSL absorbed dose heterogeneity, which is discussed further in Section 4.1.

2.4. EPR dosimetry

MCNP simulations could be used to calculate dose-rates, however we would have needed to make a number of approximations to achieve this, e.g. as the energy spectrum of the X-ray source is unavailable, we would have had to approximate it. Instead, we calculate the dose rate by determining the X-ray irradiation time required to yield the equivalent EPR signal as a known gamma dose.

Aliquots of the KRG113 samples were irradiated with a known dose at the Ecole Polytechnique Fédérale de Lau-

sanne (EPFL) using a ^{60}Co source (LOTUS) and measured following a single-aliquot regenerative protocol similar to that of Tsukamoto et al. (2015), where the regenerative points were obtained by irradiating the samples with the X-ray source. The heterogeneity in delivered dose during the gamma irradiation was evaluated using MCNP to be < 1 %. To avoid spurious signal induced by radicals formed by irradiation of the glass measurement tube, the tube was inverted between the X-ray irradiations and the EPR measurements, so that the part of the tube exposed to radiation was outside of the measurement chamber of the spectrometer. The γ-irradiated samples were irradiated in a glass vial before being decanted into measurement tubes. EPR measurements were performed using a Magnettech MS5000X X-band EPR spectrometer operating at low temperature (100 K) using liquid nitrogen. The acquisition was carried out using a microwave power of 5 mW, a modulation amplitude of 0.1 mT and a modulation frequency of 100 kHz. The Al and Ti centres were measured together in a single spectrum with a sweep amplitude of 31 mT, between 325 and 356 mT, for a total sweep time of 100 s, and averaged across three acquisitions. Each spectrum was repeated on three different days and averaged after rotating the sample tube by 120°, to average any anisotropic effects. Each aliquot was zeroed by administering a thermal treatment (400 °C, 4 min), as this treatment has been shown to cause negligible sensitivity changes (Tsukamoto et al. 2015; Toyoda et al. 2009). The samples were preheated at 160 °C for 4 min prior to measurement. Thermal treatments were carried out in a high precision heating unit designed for EPR sample tubes (Freiberg instruments). The Al signal was measured as the peak-to-peak amplitude from the top of the first peak (g = 2.0185) and the bottom of the 16th peak (g = 1.9928; Toyoda & Falguères 2003). The Ti signal was measured as the peak to baseline amplitude around g = 1.913, following the suggestion of Duval & Guilarte (2015; option D). Dose recovery tests for the regenerative protocol on this sample indicated an excellent dose recovery ratio, both for the Al and the Ti centres (3.3 % and 7.2 % respectively). The dose-rate of the X-ray source was calculated by evaluating the irradiation time needed by the X-ray source to reach a signal equivalent to that of the known γ dose.

3. Results

3.1. Deposition spectrum and effect of the glass tube relative to an aluminium filter

Previous work has shown that the use of a filter (typically aluminium, 200 µm) is necessary when irradiating samples directly exposed to the x-ray beam (i.e., not within a container) with a Varian VF-50J X-ray tube. This is to harden the spectrum by suppressing the low energy emission (< ~ 15 keV) that would otherwise lead to dose rate heterogeneity between quartz samples for trapped-charge dosimetry (Thomsen et al., 2006).

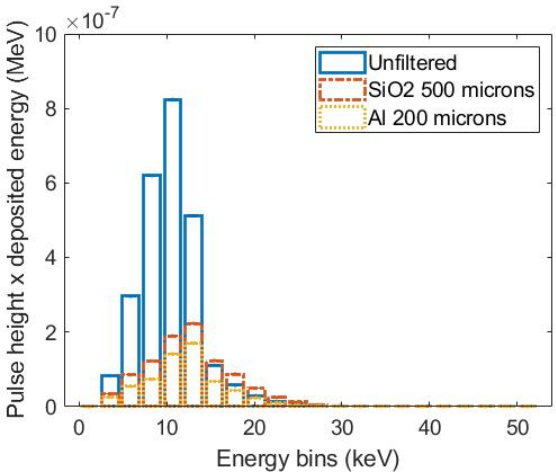

Figure 3. Energy spectrum of absorbed dose in an air cell 40 mm from the source. The spectrum was calculated for an unfiltered source (blue continuous line), a 200 µm aluminium filter (yellow dotted line), and a 500 µm glass wall (orange dashed line). The MCNP statistical errors are < 1% and cannot be discerned by eye.

The spectrum of the deposited energy was calculated at the sample position (40 mm from the source) in an air cell (1 x 1 x 0.3 cm^3) using the *F8 tally in three configurations: 1) unfiltered source, 2) 200 µm aluminium filter placed between the source and the detector and 3) 500 µm of glass between the source and the detector that replicates the wall of the sample tube. In agreement with previous studies (Fig. 2 of Richter et al. 2016), the results of these simulations indicate a strong reduction of absorbed dose between the unfiltered and filtered source at energies below ~ 15 keV (Figure 3), resulting in a general hardening of the spectrum which is similar where the source is filtered using either 500 µm of glass or 200 µm of aluminium. Furthermore, the dose rate is predicted to decrease by 63 % and 76 % for a source filtered using either 500 µm of glass or 200 µm of aluminium, respectively, compared with an unfiltered source.

These results are consistent with the GaF chromic film measurements carried out by Oppermann & Tsukamoto (2015), who estimated that absorption caused by a glass tube is ca 60 % of the unfiltered energy. The predicted reduction in dose rate is also comparable with the calculations of Andersen et al. (2003), who predicted a 50 % reduction in dose for 500 µm of SiO_2 (half-layer value), for ~ 17 keV photons, that they calculated roughly correspond to the mean energy of a 50 keV source.

As our simulation shows that the effect of the glass wall is similar to that of the aluminium filter, in terms of spectrum hardening, the use of an aluminium filter is not necessary when irradiating quartz samples for EPR analysis. All further simulations presented in this study thus exclude the Al filter. Removal of the Al filter from the "X-ray Dose" system has the considerable benefit of avoiding an unnecessarily loss in dose-rate of 56 % which would be caused by excessive spectrum filtering through the combination of the Al filter and the glass sample tube wall.

3.2. Radiation field homogeneity

Minimum sample masses of between 30 mg up to 200 mg are required for EPR analysis. Sample tube rotation has recently been introduced in the Freiberg Instrument X-ray dose system to improve radial dose homogeneity of the X-ray beam, due to absorption. We evaluated its effectiveness by simulating dose absorption in both rotating and non-rotating tubes. To avoid heterogeneity in the absorbed dose of the material, narrow sample tubes are used which result in sample heights of between 1 cm and 3 cm. Consequently, in addition to determining the radial dependence of the absorbed dose rate, it is also essential to constrain the axial dose rate dependence (Figure 4).

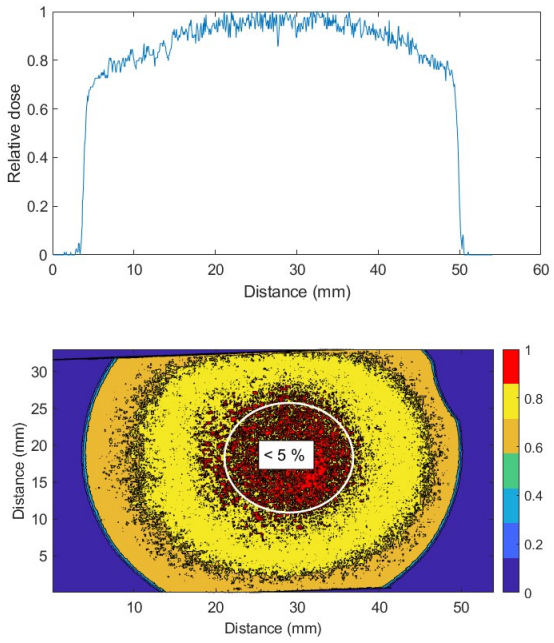

Figure 4. Mesh tallies representing a) the photon flux across a non-rotating 3 mm sample tube filled with 200 µm diameter quartz grains. The photon flux is visualised using the MCNP6 Mesh tally 1 for photons only. b) Absorbed dose across a non-rotating 3mm sample tube filled with 200 µm diameter quartz grains. The absorbed dose in each mesh cell was calculated using the MCNP mesh tally 3, equivalent to the F6 tally.The values indicated are MCNP normalised values per particle.

3.2.1 Radial dependence

Variation of deposition spectrum: The deposition of energy changes across the tube in the radial direction, as the beam is attenuated. Therefore, the deposited energy spectrum also changes across the tube as the lowest energies are progressively absorbed. In this section, we explore axial changes in the deposited energy; drastic changes in the energy deposited would require correction. As shown in Figure 5, whilst the peak in the energy spectrum for a 200 µm diameter grain located closest to the glass wall (i.e. at a median distance of 100 µm) is around ~20 keV, it is shifted to ~28 keV for a grain of the same diameter farthest from the source (900 µm). Grains farthest from the source are also exposed to an energy spectrum with a less pronounced energy peak. The mean deposited energy is, however, relatively similar between grains: ~24.8 keV for the grain closest to the source and ~26.2 keV for the grain farthest from the source.

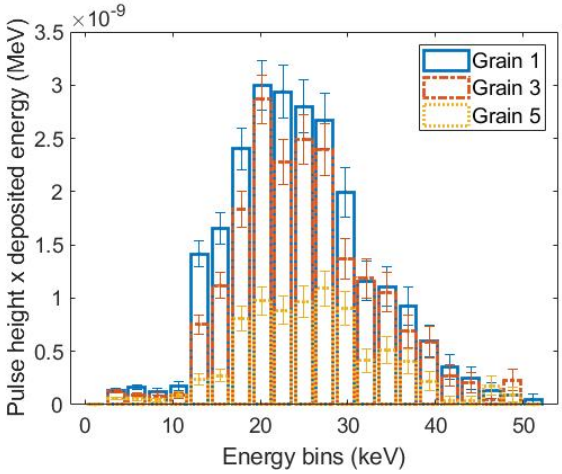

Figure 5. Variation in absorbed dose in each grain along the beam axis for a rotating sample tube. The absorbed dose in each grain was normalised by the absorbed dose in the grain closest to the glass wall (and the source). The profile was calculated for two different grain sizes: 250 µm diameter (orange dashed line) and 100 µm diameter (blue dotted line). The errors shown are the MCNP statistical errors only.

Across-tube dose attenuation: Mesh tallies were used to offer a visual representation of the distribution of absorbed dose across the tube for a non-rotating sample. Figure 6a shows the photon flux, calculated using Mesh tallies of type 1 (flux), equivalent to the F4 tally in MCNP. As expected, there is a strong dose gradient across the geometry. The spatial distribution of the absorbed dose for a non-rotating sample was evaluated using the MCNP mesh tally 3, equivalent to the F6 tally, and a visual representation is shown in Figure 6b. The distribution in absorbed dose is highly heterogeneous across the sample tube, with a reduction in absorbed dose of 70 %; this result emphasises the importance of rotating the sample during irradiation.

The variation in absorbed dose across the tube for a rotating sample was evaluated by averaging the absorbed dose in a grain with its opposite grain on the axis along the beam. The resulting profile was then normalised to the first grain closest to the source to better evaluate the proportion of absorption across the tube (Figure 7). For these calculations, the F6 tally was employed as it was found that the *F8 tally could not yield a statistically satisfactory answer, presumably due to the small size of the detector grains. Figure 7

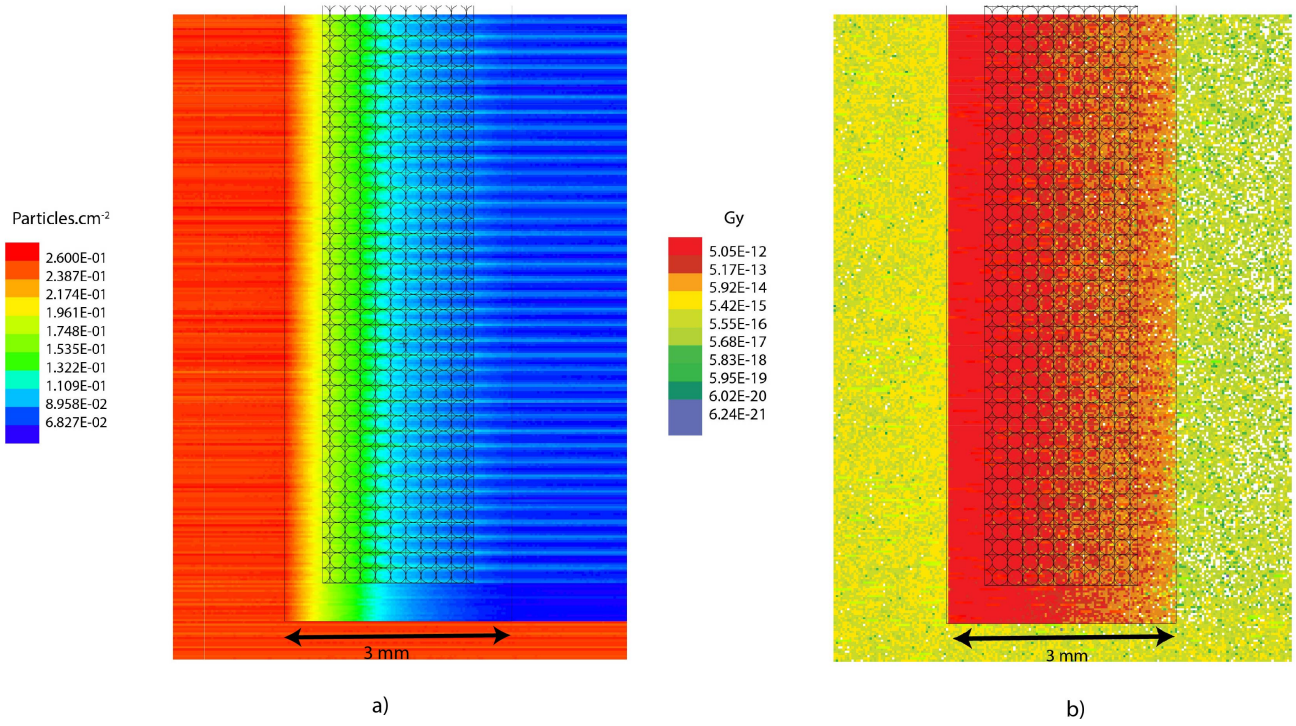

Figure 6. Axial heterogeneity in dose as evaluated by irradiating GaF radiochromic film and processing the image using the red component. The data points were normalised by the maximum measured dose, at the centre of the beam. Top graph: profile along the x-axis at the centre position. The top figure is for illustrative purposes only. Small displacements of the film can occur, and cause the offset of the maximum value from the centre. Bottom graph: full map of the 2D spatial heterogeneity. The white circle indicates the region within which the reduction in dose is less than 5 %. To achieve a more homogeneous irradiation, the sample has to be positioned within the "<5 %" circle. This is done using a positioning screw placed underneath the sample tube.

shows the profile in absorbed dose across the tube for two grain size fractions (100 and 250 µm). Although there seems to be a slight reduction in absorbed dose for different grain sizes in the range 100 – 250 µm, with a reduction of 30 and 26 % at the centre of the tube respectively, this variation can be considered as negligible, within uncertainties. Thus, on average for grains between 100 – 250 µm diameter, a 28 % decrease at the centre of the tube, compared with grains located by the glass wall is observed. This equates to a mean absorbed dose in the sample of ca 83 % of the given dose.

3.2.2 Axial dependence

The axial variation in dose was measured using GaF radiochromic film. Although the films were not calibrated for an absolute assessment of the dose, they provide an estimate of the relative variation in dose across the beam. The image was processed using Matlab. These measurements indicate that the threshold of satisfactory dose homogeneity, arbitrarily chosen to be < 5 % variation, was obtained over a sample height of 2.4 cm (Figure 4). This was thus set as the maximum height of samples for irradiation, with the lowest extent of the sample tube position fixed at the bottom of the < 5 % inhomogeneity zone. These values are slightly better than those reported by Oppermann & Tsukamoto (2015), who found relative dose variations of ca. 5.6 % within a height of 2 cm in their setup.

4. Model validation and calibration

EPR measurements were used to calibrate the X-ray source for grains of quartz in the fraction 180 – 225 µm, and luminescence measurements were used to experimentally assess the X-ray source radiation field radial divergence. Sample heights did not exceed 2.4 cm to ensure axial X-ray source heterogeneity in the absorbed dose was limited to < 5% (see Section 3.2.2). Luminescence measurements were performed by irradiating grains of quartz with the X-ray source for 100 s and measuring the resulting absorbed dose using a single-grain SAR protocol tailored for quartz (see Section 2.3 for experimental details). EPR dosimetry measurements were conducted by irradiating previously zeroed quartz samples with a known γ dose (350 $\pm$ 12 Gy to quartz; ^{60}Co LOTUS source, EPFL, Lausanne, Switzerland) and evaluating the X-ray equivalent γ dose using a SAR protocol, employing the X-ray source for the regenerative data points.

Sample name	Measured over-dispersion X-ray irradiated sample (%)	Measured over-dispersion β irradiated dose-recovery tests (%)	Accepted grains β-irradiated (%)	Accepted grains X-ray irradiated (%)	β dose recovery ratio
RisøCalQz$_{0Gy}$	31.1	7.6	79.7	30.6	1.01 ± 0.009
NUS18	32.9	8.0	90.1	21.5	1.03 ± 0.009

Table 2. Over-dispersion obtained from two quartz samples (RisøCalQz0Gy, NUS18). For the X-ray irradiated data, the samples were irradiated for 100 s in an EPR sample tube using the X-ray source operating at 50 kV, 1mA. For the β irradiated data, the samples were irradiated with 11.8 ± 0.9 Gy in a Risø TL-DA-20 instrument. For both the X-ray and β irradiated data, the subsequent doses were determined using an OSL single-grain SAR measurement procedure.1200 grains were measured for single-grain measurements.

4.1. Evaluating the heterogeneity: an experimental approach

The MCNP calculations predict heterogeneity in absorbed dose between grains irradiated within a tube; this heterogeneity should be visible as extrinsic over-dispersion in single-grain luminescence measurements. Samples RisøCalQz0Gy and NUS18 were used for single-grain measurements, sample KRG113 unfortunately has luminescence properties unsuitable for dose assessment, mainly due to a poor luminescence signal-to-noise ratio, as is typical for bedrock quartz. In contrast, the EPR properties of KRG113 were suitable for dose assessment and this sample is used for EPR calibration of the X-ray source in the next section.

Aliquots of 2 cm in height of samples NUS18 and RisøCalQz$_{0Gy}$ were irradiated in the X-ray source setup (100 s, 50 keV, 1 mA); the aliquot size was chosen to minimise the radial heterogeneity. The OSL measurements were done specifically to obtain a measurement of the dose heterogeneity, rather than absolute doses, and were done using a single-grain SAR protocol. The over-dispersion in the X-ray irradiated samples was compared with the over-dispersion of the β dose recovery test, performed on different aliquots (Table 2, Section 2.3) and is shown in Figure 8. The over-dispersion obtained from the β dose-recovery test is intrinsic to our TL/OSL reader, the sample and single-grain measurements (i.e., to the method; loss or gain of counts from the PMT, beta source heterogeneity, reproducibility of single-grain measurements due laser positioning, see Thomsen et al. 2005). In contrast, the over-dispersion measured for grains irradiated in the X-ray source setup is a combination of extrinsic over-dispersion from heterogeneity of the X-ray radiation field and the intrinsic single-grain measurement over-dispersion. As is illustrated in Figure 8, a far greater dispersion is observed for the X-ray irradiated samples.

4.2. EPR calibration

Three aliquots of ^{60}Co irradiated KRG113 were measured using EPR measurement techniques and the dose evaluated using a SAR protocol, such as described in Section 2.4 The regenerated dose response curve was found to be linear in the dose range considered (< 515 Gy) and thus was fitted with a linear function onto which the γ-induced signal was interpolated.

The EPR calibration gave dose-rate values in close agreement between the Al and Ti centres of 0.206 ± 0.008 Gy·s^{-1} and 0.206 ± 0.009 Gy·s^{-1} respectively. The uncertainty indicated here is simply the standard error derived from the three aliquots measured. However, as highlighted by the modelling results, this error does not describe the full dose-rate heterogeneity, which will be discussed in the following section.

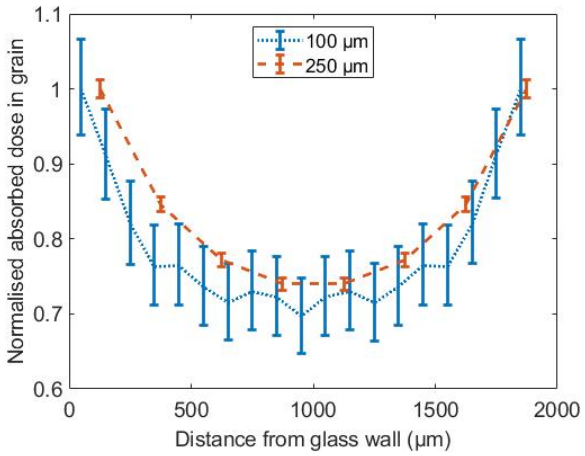

Figure 7. Deposited energy spectrum for 200 µm diameter quartz grains centred 100 µm from the glass wall (grain 1), 500 µm (grain 3) and 900 µm (grain 5) for a non-rotating sample tube. The errors shown are the MCNP statistical errors only.

5. Discussion

The energy spectrum calculated here predicts a peak X-ray dose deposition in air at photon energies between 10 and 12 keV for an unfiltered X-ray source and between 12 and 14 keV for an X-ray source filtered by either 200 µm thick aluminium or 500 µm thick glass. In our study, we have stimulated the energy deposition spectrum in air, at the location of the sample, whereas previous studies such as Thomsen et al. (2006) have stimulated the energy emitted by the source. It is expected that the energy spectrum presented in this study yields a lower emission peak. Therefore, our peak absorption value is consistent with the peak emission of ~ 20

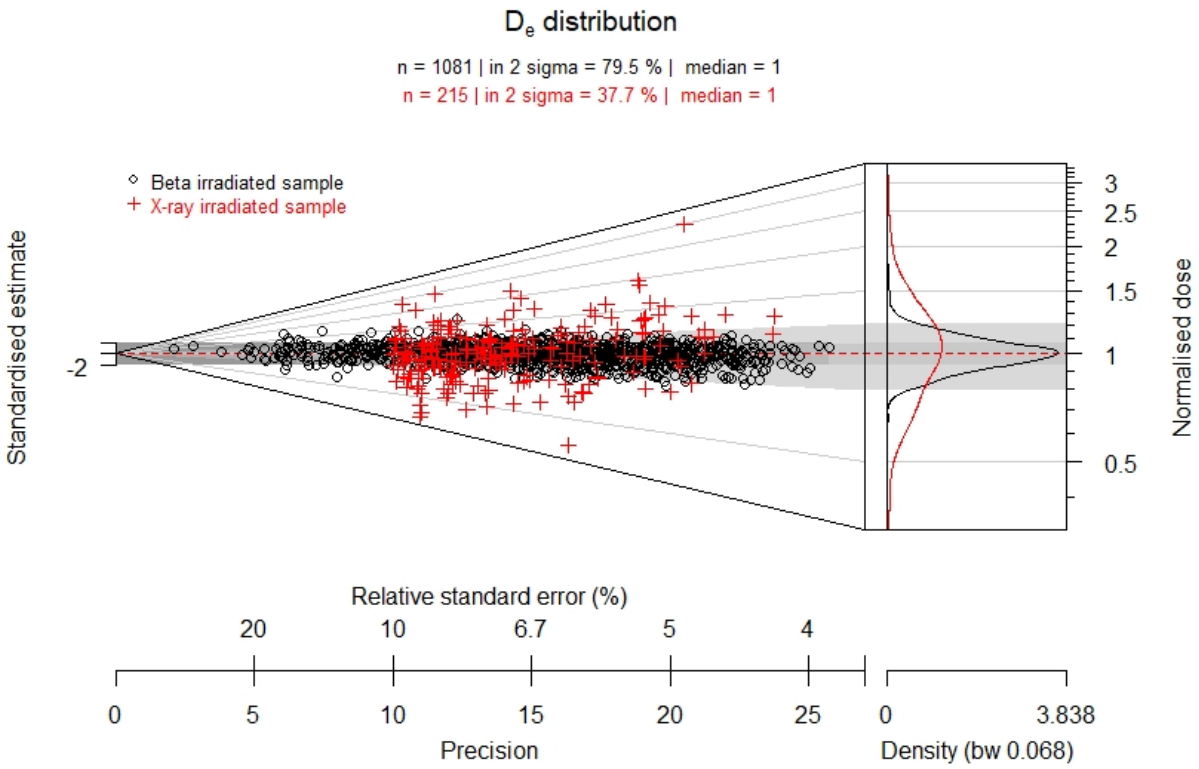

Figure 8. Abanico plot of measured equivalent doses for NUS18 samples irradiated using the X-ray source (black crosses) and using the Risø TL-DA-20 luminescence reader built-in β source (open red circles, as part of the dose-recovery test). The doses were normalised to the median dose of each dataset to allow easier visualisation of the spread in distribution.

keV reported by Thomsen et al. (2006). Furthermore, it is also close to the peak absorption value of ~ 15 keV proposed by Richter et al. (2016), where the X-ray emission and absorption spectra were calculated using Kramer's rule. Andersen et al. (2003) used Kramer's law for a thick target to calculate the mean emission energy for an unfiltered source and obtained a mean energy of ~ 17-19 keV. However, both our approach and Andersen's approach make a number of assumptions (e.g., thickness of the target, classical approximation in Andersen's case; exact emission spectrum of the source in our case). Furthermore, the precision of the predicted energy maximum is limited in our calculations by the size of the simulation bin width (2.38 keV). Simulations using smaller energy bins did not, however, yield satisfactory statistical checks for the maximum number of particles run (2.1×10^9).

The simulation results presented here validate the prediction of Richter et al. (2016), that the glass wall of the sample tube has the same effect as a 200 µm aluminium filter and therefore that the latter is not necessary when irradiating quartz samples in a glass tube. This finding is important as removing the Al filter results in an increase in the effective dose rate of 35 %, significantly accelerating sample throughput within the laboratory. This is especially significant for EPR measurements that are often applied to mid-early Pleistocene samples with absorbed doses far beyond the saturation limits of most luminescence dating methods (Rink et al., 2007).

Simulations of the axial and radial absorbed dose heterogeneity revealed considerable spatial variations. GaF film measurements showed that EPR samples irradiated in the Freiberg Instruments X-ray dose system that exceed 2.4 cm in height will have dose rate heterogeneity of > 5 % (Figure 4), whilst quartz grains measured in 3 mm diameter tubes experience a radial dose heterogeneity of ca. 28%, as predicted by MCNP, due to the attenuation of low energy X-rays throughout the sample's tube.

Although there is considerable over-dispersion in absorbed doses for samples irradiated in this setup, as assessed using luminescence single-grain measurements, the dose distribution should, in principle, be reproducible from one irradiation to another. This is confirmed by the small standard error in dose-rate between the three gamma-irradiated aliquots (< 3 %), measured using EPR to calibrate the X-ray source, where samples were repeatedly irradiated with the X-ray source to regenerate the dose points of a SAR protocol.

However, this uncertainty does not address potential variability in the strength and dose response of EPR signals between grains (Beerten et al., 2003). Indeed, if EPR signals are largely variable between grains, the EPR signal registered following irradiation of a sample would not be representative of the dose distribution across the sample tube – but rather

would be biased towards the grains exhibiting a stronger signal. However, as the grain by grain heterogeneity in EPR response is unquantified and may vary between samples, and as a large number of grains are irradiated and measured each time (tens to hundreds of mg), we have not accounted for this potential heterogeneity in our error estimates.

Nevertheless, a recommendation that can be derived from the apparent inherent dose distribution would be to avoid creating subsets of the sample following irradiation in this setup, at the risk of having an unknown dispersion in dose in the grains of the resulting samples. We note that using a hardening filter would increase the mean energy of the beam, and thus reduce the heterogeneity, whilst reducing the overall dose rate. Finally, the tube diameter is crucial, as a larger diameter would mean stronger attenuation across the tube, hence a higher radial heterogeneity.

Much recent trapped charge dosimetry research has focussed on feldspar minerals. Preliminary modelling results show that feldspar samples irradiated in the exact same setup, and without a hardening filter, as described here will show a higher absorption than quartz (76 % vs 65 % absorption across a non-rotating sample tube respectively). Thus, radial heterogeneity will be greater, yielding a lower effective dose-rate. Therefore, all the considerations summarised in this article, as well as the dose-rate measured here should not be translated to the irradiation of feldspar samples.

6. Conclusion

Using a combination of MCNP simulations, GaF film and single-grain luminescence measurements, we have shown that the irradiation of EPR samples in 3 mm diameter glass tubes using a filtered 50 keV X-ray source is inherently heterogeneous, even for samples that rotate throughout irradiation. The absorbed dose measured using EPR following irradiation is thus an average of the dose across the sample tube, assuming uniform grain response. Our simulations indicate that the use of an aluminium filter (200 µm) is redundant with the use of glass sample tubes (500 µm wall thickness), as the two materials yield similar X-ray spectrum hardening. Therefore, we refrained from using an aluminium filter in the experimental part of our study.

The dose-rate of our X-ray source to grains of quartz in the fraction 180 – 212 µm was measured using EPR dosimetry to be 0.206 ± 0.005 Gy·s^{-1}, averaging the dose-rate values for the Al and Ti centres together. It is, however, an average dose of the distribution in dose across the tube, that would be bound to change for tubes of smaller/larger diameter. The MCNP results indicate that this dose-rate is also valid for grains in the finer fraction (100 – 250 µm). The calculated dose-rate assumes a homogeneous – or at least reproducible – response between grains within an aliquot; i.e. that grain response is evenly distributed spatially, resulting in effective dose averaging. The small standard error between the three aliquots measured seems to indicate that this is the case, at least for this sample.

Acknowledgements

The authors wish to thank Shigeru Sueoka (Japan Atomic Energy Agency) and Takahiro Tagami (Kyoto University) for facilitating the field trip during which the sample KRG113 was collected and Simon Armitage (Royal Holloway) for providing the sample NUS18. Daniel Richter is acknowledged by the authors for providing the emission spectrum. The authors would also like to thank Pavel Frajtag, Laurent Braun, Daniel Godat and the EPFL LOTUS group for providing access to the ^{60}Co source, setting up the irradiation geometry and the calibration of the source.

This research was supported by funding from the European Research Commission (ERC) under the European Union's Horizon 2020 research and innovation programme, grant number 851614. The authors are also greatly thankful to Melanie Bartz for her suggestions and proofreading on the manuscript, and Federico Geser for his help with Monte-Carlo simulations.

References

Andersen, C. E., Bøtter-Jensen, L., and Murray, A. S. *A mini X-ray generator as an alternative to a 90Sr/90Y beta source in luminescence dating*. Radiation Measurements, 37(4-5): 557–561, 2003.

Autzen, M., Guérin., Murray, A. S., Thomsen, K. J., Buylaert, J. P., and Jain, M. *The effect of backscattering on the beta dose absorbed by individual quartz grains*. Radiation Measurements, 106: 491–497, 2017.

Bailiff, I. K. *An examination of beta dose attenuation effects in coarse grains located in sliced samples*. Radiation Measurements, 120: 188–194, 2018.

Beerten, K. and Stesmans, A. *ESR dating of sedimentary quartz: possibilities and limitations of the single-grain approach*. Quaternary Geochronology, 2(1-4): 373–380, 2007.

Beerten, K., Pierreux, D., and Stesmans, A. *Towards single grain ESR dating of sedimentary quartz: first results*. Quaternary science reviews, 22(10-13): 1329–1334, 2003.

Bøtter-Jensen, L., Bulur, E., Duller, G. A. T., and Murray, A. S. *Advances in luminescence instrument systems*. Radiation Measurements, 32(5-6): 523–528, 2000.

Duller, G. A. T., Bøtter-Jensen, L., and Murray, A. S. *Optical dating of single sand-sized grains of quartz: sources of variability*. Radiation Measurements, 32(5-6): 453–457, 2000.

Duval, M. and Guilarte, V. *ESR dosimetry of optically bleached quartz grains extracted from Plio-Quaternary sediment: Evaluating some key aspects of the ESR signals associated to the Ti-centers*. Radiation Measurements, 78: 28–41, 2015.

Goorley, T., James, M., Booth, T., Brown, F., Bull, J., Cox, L. J., Durkee, J., Elson, J., Fensin, M., Forster, R., Hendricks, J., Hughes, H., Johns, R., Kiedrowski, B., Martz, R., Mashnik, S., McKinney, G., Pelowitz, D., Prael, R., Sweezy, J., Waters, L.,

Wilcox, T., and Zukaitis, T. *Initial MCNP6 release overview*. Nuclear Technology, 180(3): 298–315, 2012.

Götze, J. and Lewis, R. *Distribution of REE and trace elements in size and mineral fractions of high-purity quartz sands*. Chemical Geology, 114(1-2): 43–57, 1994.

Hansen, V., Murray, A., Buylaert, J. P., Yeo, E. Y., and Thomsen, K. *A new irradiated quartz for beta source calibration*. Radiation Measurements, 81: 123–127, 2015.

Kook, M. H., Murray, A. S., Lapp, T., Denby, P. H., Ankjærgaard, C., Thomsen, K., Jain, M., Choi, J.-I., and Kim, G. *A portable luminescence dating instrument*. Nuclear Instruments and Methods in Physics Research Section B: Beam Interactions with Materials and Atoms, 269(12): 1370–1378, 2011.

Murray, A. S. and Wintle, A. G. *Luminescence dating of quartz using an improved single-aliquot regenerative-dose protocol*. Radiation Measurements, 32(1): 57–73, 2000.

Oppermann, F. and Tsukamoto, S. *A portable system of X-ray irradiation and heating for electron spin resonance (ESR) dating*. Ancient TL, 33: 11–15, 2015.

Pelowitz, D. B. *MCNP6 user's manual version 1.0*. LANL Report: LA-CP-, pp. 13–00634, 2013.

Richter, D., Mittelstraß, D., Kreutzer, S., Pintaske, R., Dornich, K., and Fuchs, M. *A new fully integrated X-ray irradiator system for dosimetric research*. Applied Radiation and Isotopes, 112: 122–130, 2016.

Rink, W. J., Bartoll, J., Schwarcz, H. P., Shane, P., and Bar-Yosef, O. *Testing the reliability of ESR dating of optically exposed buried quartz sediments*. Radiation Measurements, 42(10): 1618–1626, 2007.

Thomsen, K. J., Murray, A. S., and Bøtter-Jensen, L. *Sources of variability in OSL dose measurements using single grains of quartz*. Radiation Measurements, 39(1): 47–61, 2005.

Thomsen, K. J., Bøtter-Jensen, L., Denby, P. M., and Murray, A. S. *Luminescence response to irradiation using mini X-ray generators*. Nuclear Instruments and Methods in Physics Research Section B: Beam Interactions with Materials and Atoms, 252(2): 267–275, 2006.

Toyoda, S. and Falguères, C. *The method to represent the ESR signal intensity of the aluminium hole center in quartz for the purpose of dating*. Advances in ESR applications, 20: 7–10, 2003.

Toyoda, S., Miura, H., and Tissoux, H. *Signal regeneration in ESR dating of tephra with quartz*. Radiation Measurements, 44(5-6): 483–487, 2009.

Tsukamoto, S., Toyoda, S., Tani, A., and Oppermann, F. *Single aliquot regenerative dose method for ESR dating using X-ray irradiation and preheat*. Radiation Measurements, 81: 9–15, 2015.

Reviewers

Daniel Richter and Dirk Mittelstraß